

AN EMBEDDED-CRACK FINITE ELEMENT APPROACH TO QUASI-BRITTLE FRACTURE

G. BOLZON and A. CORIGLIANO

*Department of Structural Engineering, Politecnico of Milano
20133 Milano, Italy*

ABSTRACT

A finite element approach based on the definition of enriched displacement fields through the introduction of discontinuous interpolation functions is proposed, to the ultimate purpose of reducing the analysis of quasi-brittle fracture to a discretized problem formulated in terms of interface variables only. Beyond avoiding the need of any remeshing or inter-element boundary realignment strategy, the proposed approach allows to reduce the computation burden and to discuss about stability and bifurcation of the fracture processes.

KEYWORDS

Quasi-brittle fracture, finite element method, embedded-crack formulation, interface variables.

INTRODUCTION

Many structural problems require to consider the appearance and the evolution of important concentrate damage phenomena which cause local ruptures and material decohesion. These local phenomena can develop in macroscopical fractures across separation surfaces (henceforth called *interfaces*) embedded in one body which can be considered still in the elastic regime. Debonding and delamination of composites, fracture of quasi-brittle materials like concrete and masonry, post-localization processes are amenable of the above schematization. The progressive damage which concentrates along an interface can be simulated through a *softening* interface constitutive law, described by a relationship between tractions and displacement discontinuities, representing the cohesion between surfaces initially in contact which gradually vanishes as the complete separation is reached.

Various situations can be devised, such as frames with softening hinges, fiber debonding and composite delamination, where interfaces can be assumed to be *a priori* known. These cases are suited to the numerical approach proposed by Bolzon and Corigliano (1996), according to which the spatially discretized model of the system is derived from a weak formulation of the governing equations, and all interface fields (i.e. tractions, displacement discontinuities and internal variables governing the irreversible decohesion process) are modelled in a mixed finite element context, based on the notion of generalized variables. The resulting discrete

formulation, in the interface variables only, has been shown to be particularly advantageous both for the computational burden and for the study of uniqueness and stability of the rate problem which are not guaranteed in the presence of softening as known since Maier's work, see e.g. Maier (1968).

In other types of quasi-brittle fracture, e.g. in mixed mode fracture of specimens and structures, the location of the displacement discontinuity loci is to be determined by the numerical analyses. To this purpose and within the finite element context, various remeshing strategies have been proposed to align inter-element boundaries with fracture surfaces, see e.g. Wawrzynek and Ingraffea (1987), Bocca et al. (1991), Larsson et al. (1993).

More recently, the use of enriched finite elements with embedded displacement discontinuity surfaces has been pursued among others by Simo et al. (1993), Lotfi and Shing (1995), Larsson and Runesson (1996). The same kind of approach is followed here but, as a main difference with respect to the existing literature, the enriching discontinuous displacement field is governed by variables which are not intended to be condensed at the element level to preserve the standard displacement topology, as done elsewhere; on the contrary, the proposed *embedded-crack* formulation aims to reduce the problem to interface variables only, in order to maintain the advantages already listed above.

PROBLEM FORMULATION

Let us consider a linear elastic body Ω which can be crossed by one set Γ of interfaces Γ_i . Each interface is thought to divide the body Ω into the portions Ω^+ and Ω^- , and Ω' is defined as $\Omega' \equiv \Omega \setminus \Gamma$. The problem to be solved is that of finding the equilibrium configuration(s) of the body Ω under assigned body forces $\bar{\mathbf{b}}$ in Ω , surface loads $\bar{\mathbf{t}}$ on $\partial\Omega$, and displacements $\bar{\mathbf{u}}$ on $\partial\Omega_u$. Let \mathbf{w} and \mathbf{t} respectively represent the displacement jump and the cohesive (bridging) tractions across the interfaces. The displacement discontinuity \mathbf{w} can be splitted into its reversible and irreversible contributions, \mathbf{w}^e and \mathbf{w}^p , such that $\mathbf{w} = \mathbf{w}^e + \mathbf{w}^p$. Equilibrium can be expressed in a weak form by the virtual work principle:

$$\int_{\Omega'} \boldsymbol{\varepsilon}^T \mathbf{E} \delta \boldsymbol{\varepsilon} d\Omega' + \int_{\Gamma} \mathbf{t}^T \delta \mathbf{w} d\Gamma - \int_{\Omega'} \bar{\mathbf{b}}^T \delta \mathbf{u} d\Omega' - \int_{\partial\Omega_t} \bar{\mathbf{t}}^T \delta \mathbf{u} dS = 0 \quad \forall \delta \mathbf{u}, \forall \delta \mathbf{w} \quad (1)$$

where it has been implicitly assumed that the strains $\boldsymbol{\varepsilon}$ depend on \mathbf{u} , which is a continuous field in both Ω^+ and Ω^- , through the usual relation of compatibility in the small displacement regime, and that the stresses $\boldsymbol{\sigma} = \mathbf{E} \boldsymbol{\varepsilon}$, with \mathbf{E} representing the matrix of elastic moduli.

To complete the definition of the problem, an interface law, linking tractions \mathbf{t} to displacement discontinuities \mathbf{w} , is introduced in order to simulate the progressive damage which concentrates along Γ . The interface law may be derived from a free energy function ψ , defined per unit surface, and the irreversible behaviour can be governed by a set of static and corresponding kinematic internal variables, \mathbf{a} and $\boldsymbol{\alpha}$, as follows:

$$\dot{\mathbf{t}} = \frac{\partial \psi(\mathbf{w}^e, \boldsymbol{\alpha})}{\partial \mathbf{w}^e}; \quad \mathbf{a} = - \frac{\partial \psi(\mathbf{w}^e, \boldsymbol{\alpha})}{\partial \boldsymbol{\alpha}}; \quad (2a,b)$$

$$\dot{\mathbf{w}}^p = \frac{\partial \mathbf{f}^T(\mathbf{t}, \mathbf{a})}{\partial \mathbf{t}} \dot{\boldsymbol{\lambda}}; \quad \dot{\boldsymbol{\alpha}} = \frac{\partial \mathbf{f}^T(\mathbf{t}, \mathbf{a})}{\partial \mathbf{a}} \dot{\boldsymbol{\lambda}}; \quad (2c,d)$$

$$\dot{\boldsymbol{\lambda}} \geq 0; \quad \mathbf{f}(\mathbf{t}, \mathbf{a}) \leq 0; \quad \mathbf{f}^T \dot{\boldsymbol{\lambda}} = 0 \quad (2e,f,g)$$

In the above relations, $\mathbf{f}(\mathbf{t}, \mathbf{a})$ and $\boldsymbol{\lambda}$ respectively represent a set of convex activation functions and a vector of *plastic* multipliers. Differentiability but not convexity is required for the free energy function ψ to the purpose of reproducing softening.

The interface constitutive law can be chosen within the class of models which obey a maximum dissipation principle (Nguyen, 1993) as in the previous work by Bolzon and Corigliano (1996), to allow for the derivation of uniqueness and stability conditions for the global response.

The discrete counterpart of equilibrium equations (1) is obtained after space-discretization of the domain Ω through the use of enriched finite elements. These are defined as standard displacement-based elements at the beginning of the analysis, and are enriched by an additional incompatible displacement field, discontinuous across an embedded interface, when an activation criterion is satisfied. The enhanced displacements are described by the usual shape functions \mathbf{N}_u (with continuous space derivatives \mathbf{B}_u) interpolating the nodal displacements collected in vector \mathbf{U} , and by the discontinuous shape functions \mathbf{N}_d relevant to the discontinuities across the embedded interfaces Γ_i , collected in vector \mathbf{W} . It is important to notice that functions \mathbf{N}_d are discontinuous across Γ but continuous and derivable (with derivatives \mathbf{B}_d) in both Ω^+ and Ω^- , see e.g. Fig. 1.

The displacement and the strain fields in Ω^+ and Ω^- can then be described as:

$$\mathbf{u} = \mathbf{N}_u \mathbf{U} + \mathbf{N}_d \mathbf{W}, \quad \boldsymbol{\varepsilon} = \mathbf{B}_u \mathbf{U} + \mathbf{B}_d \mathbf{W} \quad (3a,b)$$

The opening displacements \mathbf{w} and cohesive tractions \mathbf{t} along the interface are modelled by means of the corresponding work-conjugate discrete quantities \mathbf{W} and \mathbf{T} through the interpolation functions \mathbf{M}_w and \mathbf{M}_t , respectively:

$$\mathbf{w} = \mathbf{M}_w \mathbf{W}, \quad \mathbf{t} = \mathbf{M}_t \mathbf{T} \quad (4a,b)$$

Interpolation functions \mathbf{M}_w are deduced from relation (3a) applied along Γ where $\mathbf{w} \equiv \mathbf{u}^+ - \mathbf{u}^-$. Interpolation functions \mathbf{M}_t are defined over Γ in such a way to satisfy the following scalar-product conservation property:

$$\int_{\Gamma} \mathbf{t}^T \mathbf{w} d\Gamma = \mathbf{T}^T \mathbf{W} \quad (5)$$

Substitution of (3) and (4) in the equilibrium statement (1) gives the following system of equations

$$\begin{bmatrix} \mathbf{K}_{uu} & \mathbf{K}_{ud} \\ \mathbf{K}_{du} & \mathbf{K}_{dd} \end{bmatrix} \begin{Bmatrix} \mathbf{U} \\ \mathbf{W} \end{Bmatrix} = \begin{Bmatrix} \mathbf{F}_u \\ \mathbf{F}_d - \mathbf{T} \end{Bmatrix} \quad (6a)$$

where:

$$\mathbf{K}_{uu} = \int_{\Omega'} \mathbf{B}_u^T \mathbf{E} \mathbf{B}_u d\Omega, \quad \mathbf{K}_{ud} = \mathbf{K}_{du}^T = \int_{\Omega'} \mathbf{B}_u^T \mathbf{E} \mathbf{B}_d d\Omega, \quad \mathbf{K}_{dd} = \int_{\Omega'} \mathbf{B}_d^T \mathbf{E} \mathbf{B}_d d\Omega \quad (6b,c,d)$$

$$\mathbf{F}_u = \int_{\Omega'} \mathbf{N}_u^T \bar{\mathbf{b}} d\Omega + \int_{\partial\Omega_t} \mathbf{N}_u^T \bar{\mathbf{t}} dS, \quad \mathbf{F}_d = \int_{\Omega'} \mathbf{N}_d^T \bar{\mathbf{b}} d\Omega + \int_{\partial\Omega_t} \mathbf{N}_d^T \bar{\mathbf{t}} dS \quad (6e,f)$$

Linear equilibrium equations (6) must be solved together with the discrete counterpart of the non-linear interface constitutive law. This can be simply derived in terms of the variables \mathbf{T} and \mathbf{W} since, by virtue of interpolations (4) which obey condition (5), these are related to their continuum counterparts by the following relations:

$$\mathbf{T} = \int_{\Gamma} \mathbf{M}_w^T \mathbf{t} d\Gamma \quad \mathbf{W} = \int_{\Gamma} \mathbf{M}_i^T \mathbf{w} d\Gamma \quad (7a,b)$$

The discrete counterparts of the static and kinematic internal variables which govern the irreversible behaviour of the interface through eq.s (2) can also be defined as above, see e.g. Bolzon and Corigliano (1996), and allow deriving a discretized version of the interface law, which maintains the main features of the original continuum model and which can be described as follows:

$$\mathbf{T} = \frac{\partial \Psi(\mathbf{W}^e, \boldsymbol{\alpha})}{\partial \mathbf{W}^e}; \quad \mathbf{A} = -\frac{\partial \Psi(\mathbf{W}^e, \boldsymbol{\alpha})}{\partial \boldsymbol{\alpha}}; \quad (8a,b)$$

$$\dot{\mathbf{W}}^p = \frac{\partial \mathbf{F}^T(\mathbf{T}, \mathbf{A})}{\partial \mathbf{T}} \dot{\boldsymbol{\lambda}}; \quad \dot{\boldsymbol{\alpha}} = \frac{\partial \mathbf{F}^T(\mathbf{T}, \mathbf{A})}{\partial \mathbf{A}} \dot{\boldsymbol{\lambda}}; \quad (8c,d)$$

$$\dot{\boldsymbol{\lambda}} \geq 0; \quad \mathbf{F}^T(\mathbf{T}, \mathbf{A}) \leq 0; \quad \mathbf{F}^T(\mathbf{T}, \mathbf{A}) \dot{\boldsymbol{\lambda}} = 0 \quad (8e,f,g)$$

Nodal displacements \mathbf{U} may be conveniently eliminated from (6) through static condensation, to obtain the following equation system whose dimensions are much smaller than the original size of (6):

$$\mathbf{T} = \mathbf{P}_\Gamma - \mathbf{K}_\Gamma \mathbf{W} \quad (9)$$

where: $\mathbf{K}_\Gamma = \mathbf{K}_{dd} - \mathbf{K}_{du}^T \mathbf{K}_{uu}^{-1} \mathbf{K}_{ud}$ and $\mathbf{P}_\Gamma = \mathbf{F}_d - \mathbf{K}_{du} \mathbf{K}_{uu}^{-1} \mathbf{F}_u$.

Note that matrices \mathbf{K}_{ud} , \mathbf{K}_{du} and \mathbf{K}_{dd} change their dimension depending on the number of

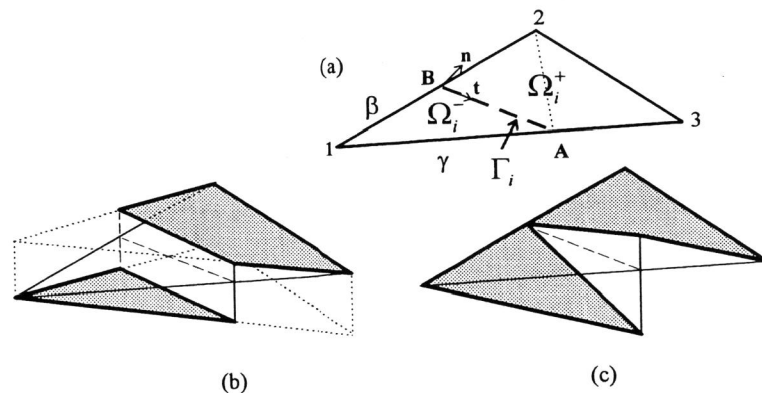


Fig. 1 A 3-node plane triangular element (a) and possible interpolation function for the enhanced displacement field, with constant (b) or linear (c) discontinuity along the interface

embedded interfaces already activated. On the contrary, matrix \mathbf{K}_{uu} is constant throughout the whole analysis since linear elastic behaviour has been assumed outside the interfaces, and therefore can be computed, and inverted, once for all at the beginning of the analysis. Equations (9) are also to be solved together with the interface law in its discrete format (8). It can be observed that the terms \mathbf{P}_Γ and $-\mathbf{K}_\Gamma \mathbf{W}$ on the r.h.s. of equations (9) respectively represent the response to the external loads and to superimposed distortions \mathbf{W} of the undamaged, perfectly bonded, linear elastic body Ω in terms of the interface tractions \mathbf{T} .

ENHANCED EMBEDDED-CRACK ELEMENT

Before activation of the embedded discontinuity surfaces, the considered finite elements behave as standard three-node constant strain (CST) plane elements with elastic behaviour. A maximum principal stress criterion ($\sigma_1 = \sigma_{cr}$) is used as activation criterion, and the embedded displacement discontinuity lines are orthogonal to the maximum tensile direction.

The interfaces Γ_i , at most one for each element, may cross the element in any position; the interface length and hence the stiffness of the enhanced element change depending on the interface position. In the present implementation, each interface can either cross the centroid of the element or follow the pre-existing cracks across the boundary of the adjoining elements. In this second case, an actual fracture surface can be visualized.

The displacement discontinuity across the embedded interface may be assumed to be constant, as schematically represented in Fig. 1(b), or to vary linearly along Γ_i as shown in Fig. 1(c). In the first case, the interpolation functions N_d^+ and N_d^- which enable to enhance the displacement field in Ω^+ and Ω^- respectively, can be defined by:

$$N_d^+ = \alpha N_1(x, y); \quad N_d^- = (\alpha - 1) N_1(x, y) \quad (10a,b)$$

where $N_1(x, y)$ represents the shape function for mode I of the standard CST element. The interpolation function M_w defined on Γ_i for opening and sliding modes, results equal to the identity in the local reference system (\mathbf{t}, \mathbf{n}) of Fig. 1(a). This kind of interpolation corresponds to that proposed by Lotfi and Shing (1995) for 4-node isoparametric plane element.

It is worth to be noticing that the strain field inside the enhanced element remains uniform also after the activation of the embedded discontinuity, and that the coefficient α in (10) does not affect the results. In fact, it can be shown that α does not enter explicitly in the analysis, and that the partition of \mathbf{w} which defines \mathbf{u}^+ and \mathbf{u}^- on Γ_i depends uniquely on the interface position, i.e. $\mathbf{u}^+ = \gamma \mathbf{w}$ in A and $\mathbf{u}^- = \beta \mathbf{w}$ in B, see Fig. 1(a) and (b).

Interpolation (10) gives piece-wise constant representation of the opening displacement, without ensuring conformity at the inter-element boundaries crossed by fracture surfaces, and the element opening/sliding behaviour results almost independent of the adjoining element stiffness. Inter-element continuity could be enforced by defining e.g.

$$N_{dA_1}^+ = \alpha_A \frac{N_2(x, y)}{\gamma}; \quad N_{dA_2}^+ = \alpha_A \frac{N_1(x, y)}{1 - \gamma}; \quad N_{dA}^- = (\alpha_A - 1) \frac{N_2(x, y)}{\gamma} \quad (11a,b,c)$$

respectively in the portions A3B and A23 of Ω_i^+ and in Ω_i^- , see Fig. 1(a).

The coefficient α_A depends in this case on the stiffness of the enhanced element as well as on the stiffness of the adjoining elements; it is generally different for opening and sliding modes and can be evaluated, if needed, as one part of the solution.

By the choice (11) the interpolation functions M_w for opening and sliding modes result, as required:

$$M_{wA} = \tau; \quad M_{wB} = 1 - \tau \quad (12a,b)$$

where the normalized parameter $0 \leq \tau \leq 1$ identifies each point of the segment BA ($\tau = 0$ in B). Further details and other possibilities to enforce inter-element continuity will be given in a forthcoming paper.

NUMERICAL TEST

The above described formulation has been implemented so far with constant displacement discontinuity along the embedded interface as shown by Fig. 1(b). The effectiveness of the implementation has been tested through the simulation of the mixed mode failure of notched plate represented in Fig. 2(a). Tension and shear deformations are prescribed simultaneously, keeping constant, equal to 1, the ratio of the vertical to the horizontal displacements. Material data are as follows: Young's elastic modulus $E = 30$ GPa, Poisson's ratio $\nu = 0.2$, tensile strength $\sigma_t = 3$ MPa, fracture energy $G_f = 100$ J/m². The assumed interface law is linear softening in mode I. The in plane geometrical data are in Fig. 2, expressed in mm.

Experimental results for this specimen have been obtained by Nooru-Mohamed (1992) and numerical simulations have been made by Lotfi and Shing (1995) and by Larsson and Runesson (1996).

The load-displacement curves of Fig. 2(b) have been obtained by the finite element discretization shown in Fig. 3. Good agreement can be found with the results of the other above quoted numerical analyses, although discrepancies with experimental work still exist.

A spread activation of the embedded interfaces has been observed at the beginning of the analysis but, although no special provision has been implemented so far to govern such an activation, many potentially active surfaces actually close in subsequent loading steps, and most damage localizes into a narrow band emanating from the left notch of the plate and develops into a straight true crack before turning sharply. This kind of behaviour resembles the experimentally observed one, but the influence of the discretization cannot be ruled out at the present time since elements outside the more refined central portion of the mesh have been defined as standard CST elements.

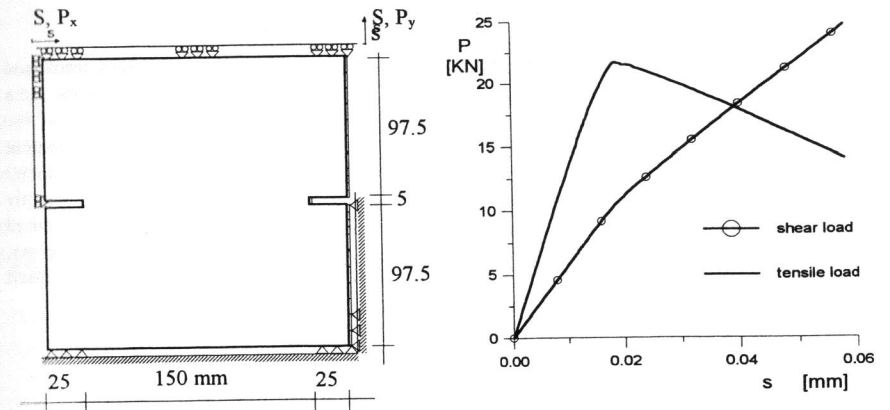


Fig. 2 Mixed mode notched specimen (a) and the load-displacement curves (b).

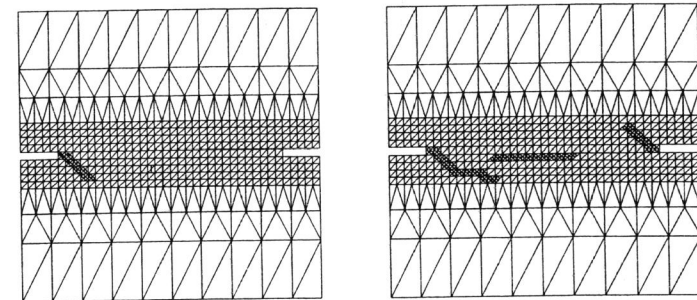


Fig. 3 Mixed-mode failure of a notched plate: the evolution of the crack surfaces; circles indicate completely damaged elements.

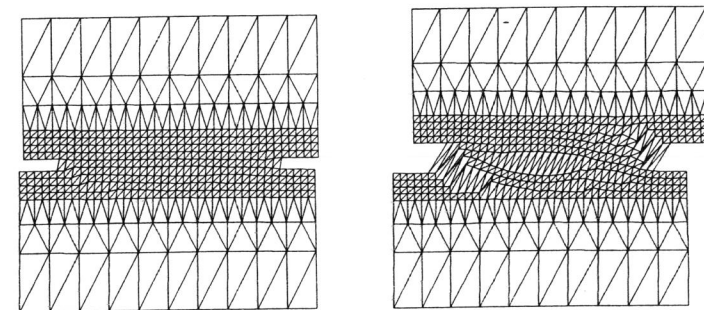


Fig. 4 Mixed-mode failure of a notched plate: deformed meshes at the beginning (left) and toward the end (right) of the fracture process.

CONCLUSION

In this paper, one formulation for quasi-brittle fracture analysis, based on embedded crack and interface variables has been presented with some encouraging although preliminary results. As a main difference with previous works, interface variables associated to the description of the embedded cracks are retained in the formulation, while the continuous part of the displacement field can be condensed to give a problem in the interface variables only. This approach allows to: reduce the size of the problem to be solved at each loading step, to derive and to apply stability and uniqueness conditions, to implement local control algorithms based on the retained displacement discontinuities. These issues are partly already implemented, partly in progress; others remain to be addressed, among which is the systematic study of the embedded-crack activation criteria and of the relevant control algorithms.

REFERENCES

- Bocca, P., Carpinteri, A. and Valente, S. (1991) Mixed mode fracture of concrete. *Int. J. Solids Structures*, **27**, 1139-1153.
- Bolzon, G. and Corigliano, A. (1996). A discrete formulation for elastic solids with damaging interfaces. *Comp. Meth. Appl. Mech. Engng*, in press.
- Larsson, R. and Runesson, K. (1996) Element-embedded localization band based on regularized displacement discontinuity. *ASCE J. Engng Mech.*, **122**, 402-411.
- Larsson, R., Runesson, K. and Ottosen, N.S. (1993) Discontinuous displacement approximation for capturing plastic localization. *Int. J. Num. Meth. Engng* **36**, 2087-2105.
- Lotfi, H.R. and Shing P.B. (1995) Embedded representation of fracture in concrete with mixed finite elements, *Int. J. Num. Meth. Engng*, **38**, 1307-1325.
- Maier, G. (1968) On softening flexural behaviour in elastic-plastic beams. *Rend. Ist. Lombardo Sci. Lett.* (in italian), **102**, 648-677.
- Nguyen, Q.S. (1993) Bifurcation and stability of dissipative systems. In: *CISM Lectures n. 327*, Udine, Springer-Verlag.
- Nooru-Mohamed, M.B. (1992) *Mixed mode fracture of concrete: an experimental approach*. PhD Dissertation, Delft University of Technology.
- Simo, J.C., Oliver, J. and Armero, F. (1993) An analysis of strong discontinuities induced by strain-softening in rate-independent solids. *Comp. Mech.*, **12**, 277-296.
- Wawrzynek, P.A. and Ingraffea, A.R. (1987) Interactive finite element analysis of fracture processes: an integrated approach. *Theor. Appl. Fract. Mech.*, **8**, 137-150.